Jül-Conf-45 D2-8

ICANS-V

MEETING OF THE INTERNATIONAL COLLABORATION ON

ADVANCED NEUTRON SOURCES

June 22-26, 1981

Measurements of Neutron Fluxes at Spallation Source Models and Bare Targets

V. Drüke, N. Paul and W. Litzow

Institut für Reaktorentwicklung der KFA Jülich GmbH

Postfach 1913, D-5170 Jülich, Germany

ABSTRACT

Thermal and fast neutron fluxes have been measured at spallation source models and bare target configurations. Different moderators and target materials have been used. The peak values of thermal fluxes were calculated from reaction rates to 9.6 10^{-3} n/cm^2 s p for H_2O, 1.4 10^{-2} n/cm^2 s p for D_2O and for the hybrid system 9.0 10^{-3} n/cm^2 s p in the case of slow moderator and 1.5 10^{-2} n/cm^2 s p in that of fast moderator. Tungsten targets gave a 20 % reduced flux, uranium targets produced by factor of 1.8 increased flux in the moderator. Fast fluxes have been measured on the surface of bare Pb and U-targets using the Rh103 (n,n') reaction. All measurements will be compared with calculations in future.

INTRODUCTION

As a part of the German study of a spallation neutron source (SNQ) /1/ neutron fluxes in the thermal and fast energy region have been measured recently. Targets consisting of lead, lead-bismuth, uranium and tungsten/lead have been bombarded by 590-MeV protons at the Schweizerisches Institut für Nuklearforschung (SIN). The produced neutrons were moderated in H_2O, PE and D_2O and the distribution of the thermal neutron flux have been measured. Using the proton beam of the SATURNE-accelerator (CEA Saclay) fast neutron distributions have been determined at surface of bare lead or uranium targets with an incident proton energy of 600 and 1100 MeV. The experimental results may give indications of the layout of a spallation source and can be compared with calculations.

EXPERIMENTAL SETUP AND PROCEDURES

Measurements of the thermal neutron fluxes were done with different moderators and target configurations. As moderators were used light water, heavy water and polyethylene and as target compositions lead, lead-bismuth, uranium and tungsten/lead in slab and cylindrical geometries (see table I).
The experimental setup of each experiment is shown in the corresponding figure.
The thermal neutron flux was determined by the measurement of reaction rate of dysprosium- and uranium detectors. Small aluminum-dysprosium wires (ϕ 0.7 x 10 mm^3) containing 10.4 % Dy were used to measure the flux distribution in the moderators. Due to the relative short half-live period of 141 min only 150 detectors could be used in one experiment at the same time. To determine the absolute flux value several uranium detectors were irradiated together with the Dy-wires. Counting the 1.6 MeV-γ-line of La 140 (fission product of U-235) the absolute reaction rate of the uranium samples was

Table I: Target Configurations and Compositions
Sizes of Moderators and Dimensions of Targets
are given in the Figures

Moderator	Target Material	Target Geometry
H_2O	Pb-Bi	cylindrical
H_2O	Uranium (depl. 0.4%)	"
D_2O	Pb	"
"	Pb-Bi	"
"	Pb	slab
"	Uranium (depl. 0.4%)	"
D_2O/PE	Pb	slab
"	"	"
"	W-Pb	"

determined. The comparison of the uranium and the Dy detectors gave the absolute reaction rate in the moderator. The conversion from reaction rate to flux has been calculated with the fission cross section of U-235. In these calculations a Maxwellian energy distribution of the thermal flux was assumed in all moderators with a corresponding fission cross section of 515 barn. The validity of this assumption has to be proved by other experiments or calculations. The counting errors from the Dy-wires can be indicated with 0.4 up to 2 % due to the time dependent γ-background in the accelerator areas. The uncertainty of the uranium detectors was about 3 % including that of the calibration standard. The uncertainty of the resulting thermal neutron flux can be given with 3.5 % not included the exact value of the fission cross section of U-235. The relative flux distribution however has a possible error of 2 % maximum.

Another uncertainty has to be remarked of the beam calibration. The proton beam was directed onto a graphite scatterer viewed by a telescope of scintillator counters operated in coincidence. The telescope was calibrated

by reducing the beam current to a level where direct counting was possible and comparing the number of coincidences recorded to the number of protons counted in the direct beam. The uncertainties of this method were estimated to be 5 up to 10 % from reproducibility obtained in different runs.
The measurements of the fast neutron flux were done by activation of rhodium foils placed on the surface of bare targets configurations. The neutron scattering cross section of rhodium 103 is shown in figure 14, the conversion from reaction rate to flux is considerably dependent on the neutron spectrum. Therefore in the corresponding figures the measured reaction rate is indicated, rather than neutron fluxes. The reaction rate has been measured with an uncertainty of 3.5 %.

EXPERIMENTAL RESULTS AND CONCLUSIONS

In figure 1 the cross section of the target configuration is shown for the H_2O and several of D_2O experiments. The cylindrical targets were surrounded by an inner aluminum tube, an air gap and an outer aluminum tube. In the case of H_2O moderators the outer tube and air gap are not present. All targets were mounted in a stainless steel tank with the dimensions of 1.7 m x 1.7 m x 1.7 m. Fig. 2 shows the response of the flux measurements in general. In the following figures only a few sections of this flux distributions parallel and perpendicular to the incident proton beam is given. Fig. 3-5 show the neutron flux space dependent as indicated on the figures in the H_2O case.
The peak flux in the case of Pb/Bi-target is given in Fig. 3 in dashed line with 3 10^7 n/cm^2 s 0.5 nA. A three times higher peak flux is obtained at a distance of 5 cm from the target surface. For the uranium target Fig. 5 shows a flux measurement with and within a beam tube.
Fig. 6 and 7 give some typical results to the D_2O measurements. Fig. 6 shows the unpertubated case with peak flux of 4.3 10^7 n/cm^2 s 0.5 nA and a FWHM of 85 cm. Fig. 7 gives an impression of the flux pertubation in the D_2O system due to beam tube arrays.

Fig. 8-13 show some results and views related to the hybrid systems with a slow and a fast moderator. Fig. 8-10 give the results of a benchmark experiment with a simple geometry: target, fast moderator PE, slow moderator D_2O. The peak flux of the Pb target in D_2O has a FWHM of 50 cm and a value of 0.94 10^7 n/cm^2 s 0.5 nA. For U-target the flux increases by a factor of 1.72. In the fast moderator the maximum of thermal flux is four times higher than in D_2O. Fig. 10 shows the flux perpendicular to the proton beam. The ratio of the flux in case of U- and Pb-target is strongly space dependent due to the properties of the target materials.

In Fig. 11 the mock up assembly of the SNQ design is illustrated. The target is diluted with sheets of PE to simulate the water cooling.

The fast moderator with grooves on the surface is reflected by PE or Pb. Fig. 12 and 13 show some results measured in this assembly. Fig. 12 shows the flux values in D_2O with a peak flux of 2.75 10^7 n/cm^2 s 0.5 nA and with a FWHM of 60 cm. The thermal flux increases by a factor of three compared to the results of measurement without "PE-coolant". This effect can be explained by reason of premoderation of neutrons in the target. In the fast moderator the premoderation causes only a flux gain of 30 %.

Other target materials than Pb were used, uranium and tungsten. Uranium increases the thermal flux by a factor of 1.8 and tungsten (without "coolant") decreases the flux within 20 % in the slow moderator. If we compare the W-target with the compact Pb-target we would get roughly a factor of 2.3 in the thermal flux in D_2O.

Figs. 15-17 show the results of fast reaction rates measured with rhodium foils on the surface of bare targets. Fig. 14 gives the inelastic scattering cross section of rhodium with a threshold energy of 0.1 MeV. A conversion from reaction rates to flux is strongly dependent of the neutron spectrum and has to be calculated.

Fig. 15 and 16 show the results of the activation at two different proton energies (600 and 1100 MeV). The different behaviour of the 100 x 300 mm^3 targets is due to the scattering from neutrons from the target sides.

Fig. 17 gives the result of different target materials for a proton energy of 1100 MeV. The measurement shows a factor of 1.7 in the peaks of U- and Pb-target. As expected the range of the protons is shorter in the uranium target than in the lead target. The integrated reaction rate over the target length gives a factor of about 2.2 between the proton energies of 1100 and 600 MeV for both target materials, lead and uranium.

ACKNOWLEDGEMENTS

The authors acknowledge the help provided during the measurements by the SIN people, especially Dr. W. Fischer and Dr. C. Tschalär, and by the LNS staff, particularly Dr. F. Faure, Dr. G. Milleret and Dr. J. Ciret.

REFERENCES

/1/ SNQ - Realisierungsstudie — JüL-Spez-113 / KfK 3175

/2/ Annual Progress Report on Nuclear Data 1980 — NEANDC (E) 222 "U" VOL. III EURATOM March 1981

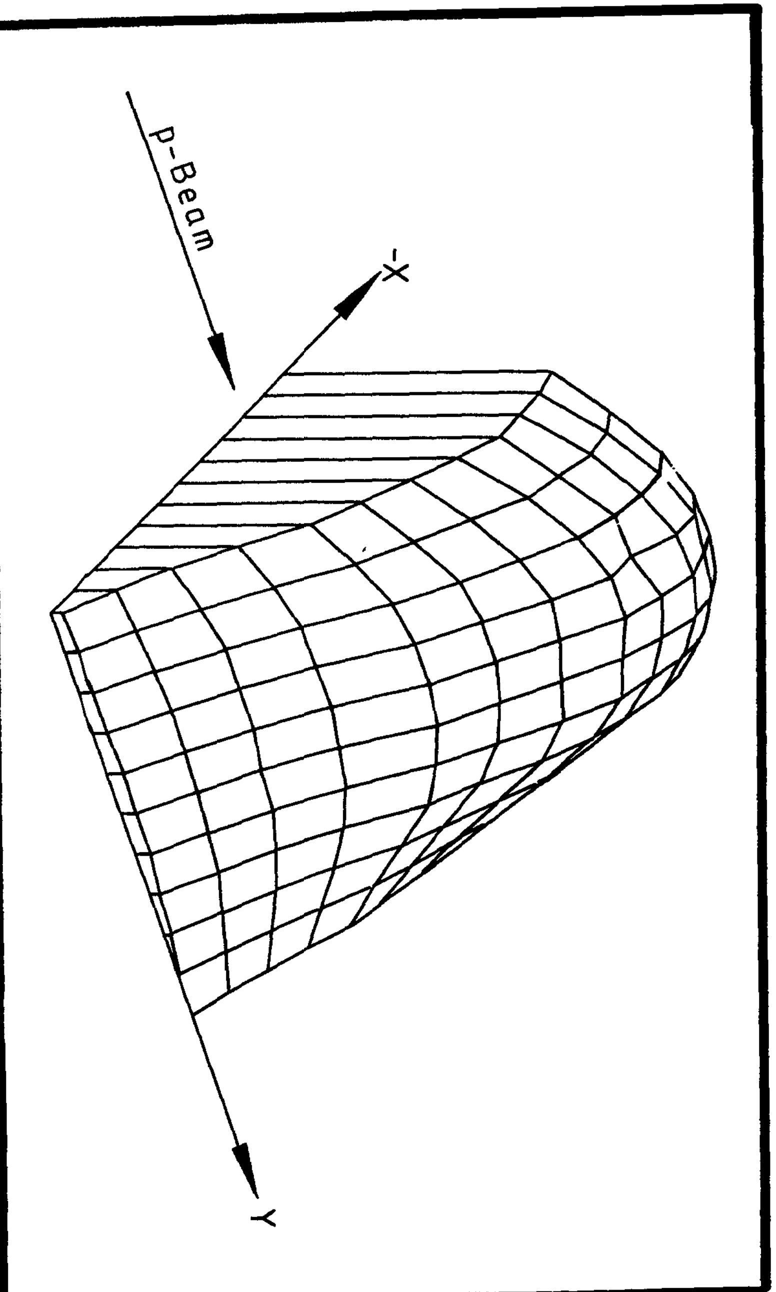

Thermal Flux in X-Y Direction

Fig.: 2

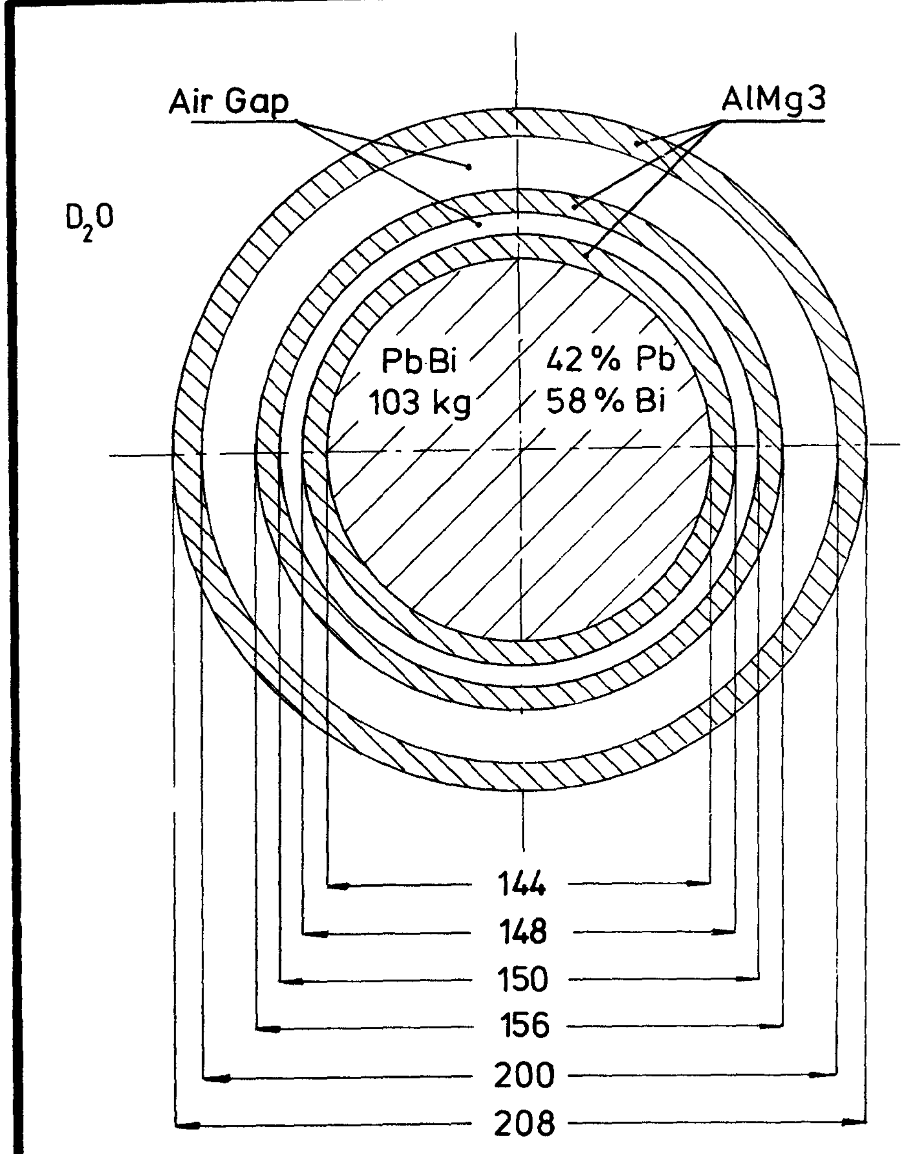

Section of the Pb Bi-Target Configuration in D_2O-Tank

Fig.: 1

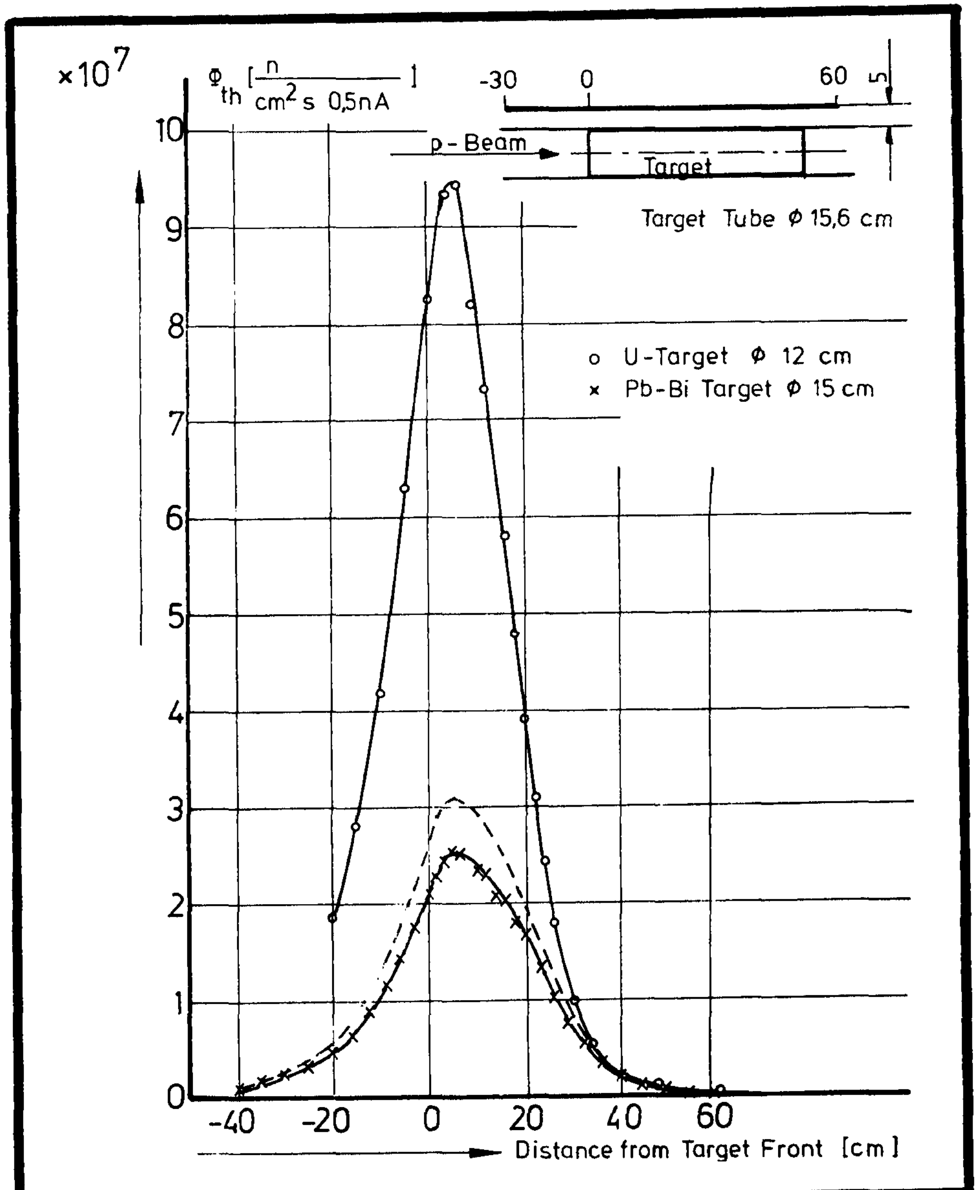

KFA | Thermal Flux, U-and Pb-Bi Target in H_2O | Fig.: 3

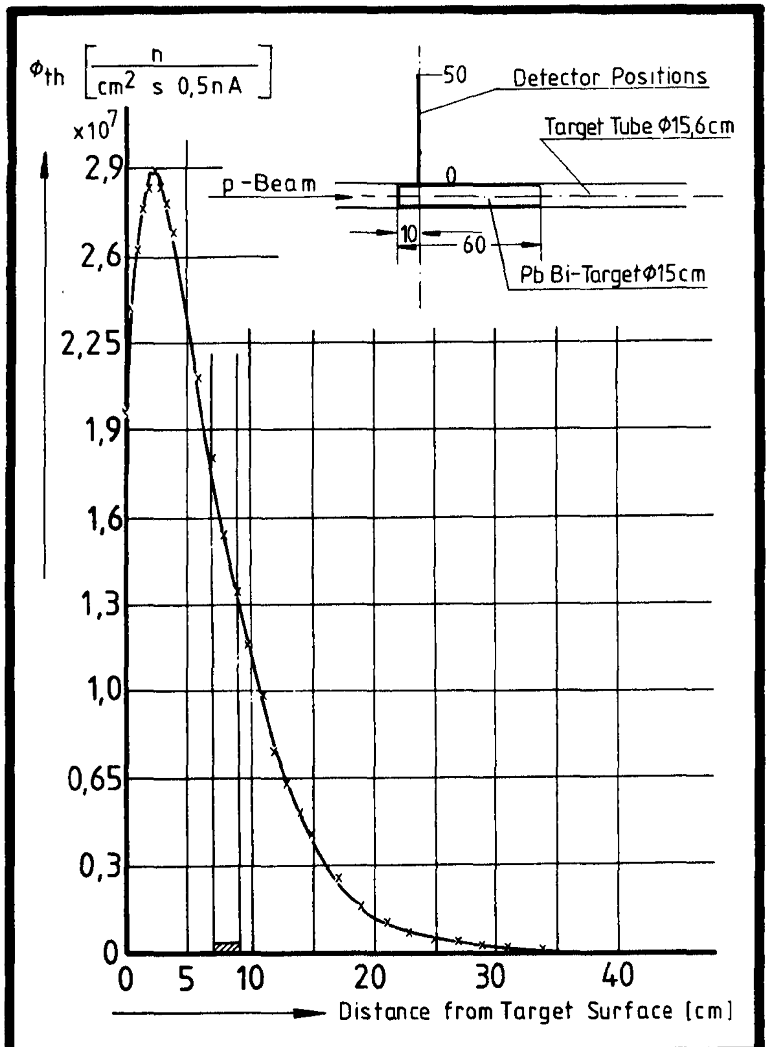

KFA | Thermal Flux PbBi-Target in H_2O | Fig.: 4

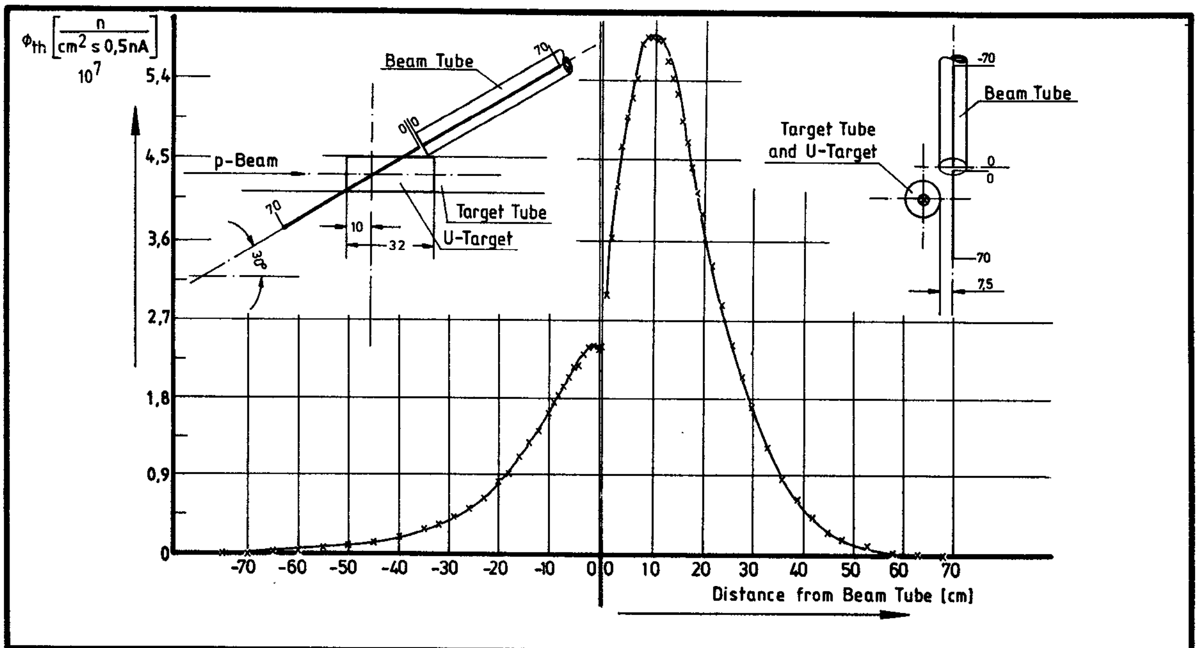

KFA | Thermal Flux U-Target in H_2O | Fig.: 5

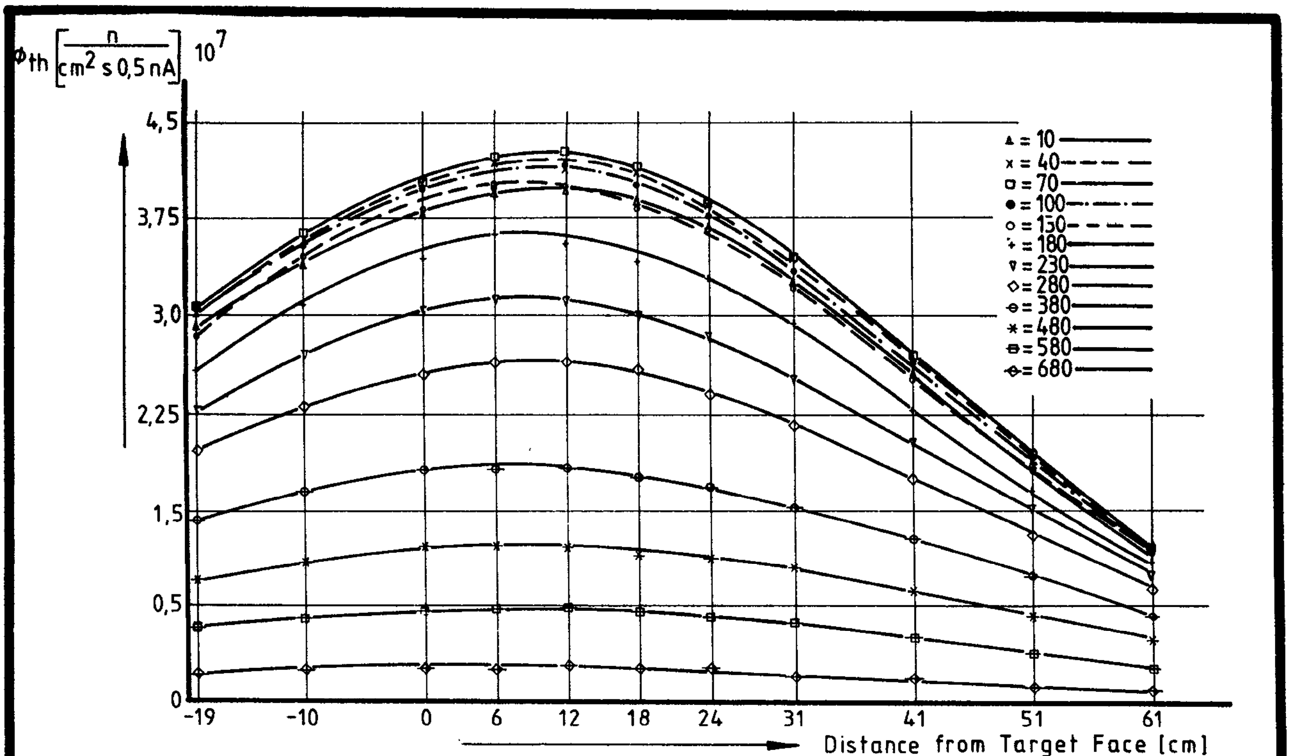

KFA | Thermal Flux in D_2O Pb-Target ; Pb Bi-Target | Fig.: 6

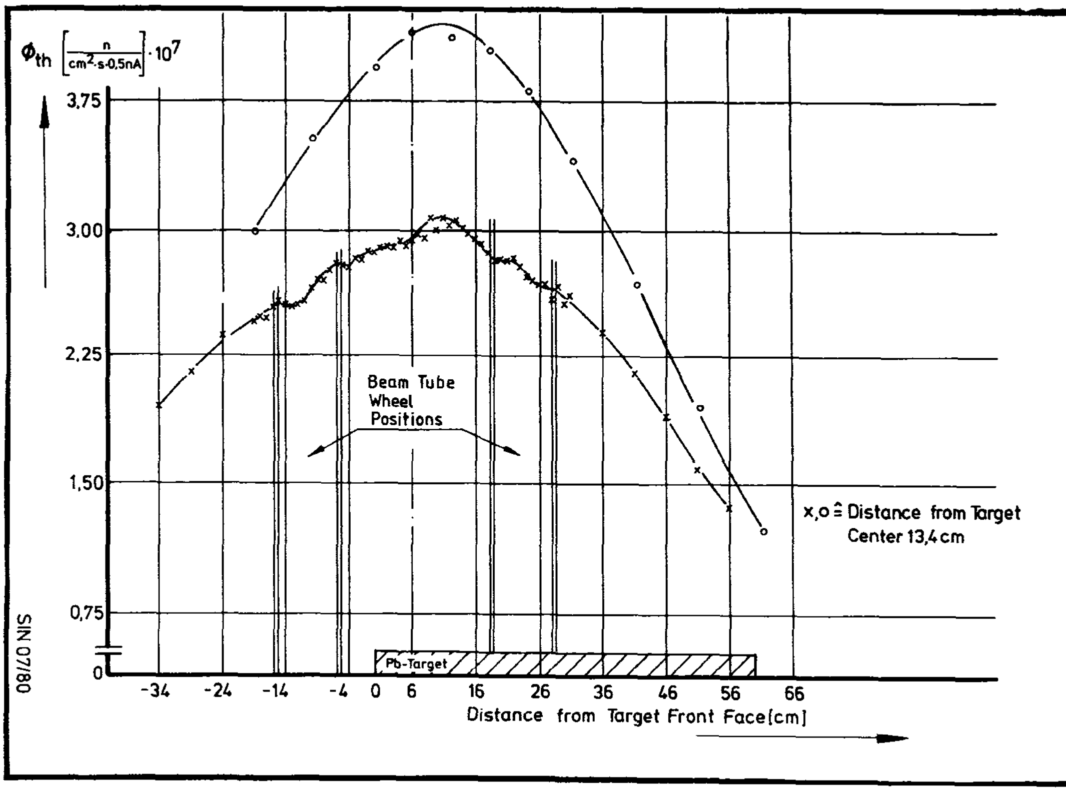

Thermal Flux in D_2O, Pb-Target ϕ15cm
o—o undisturbed
x—x disturbed by Beam Tube Wheels

KFA

Fig.: 7

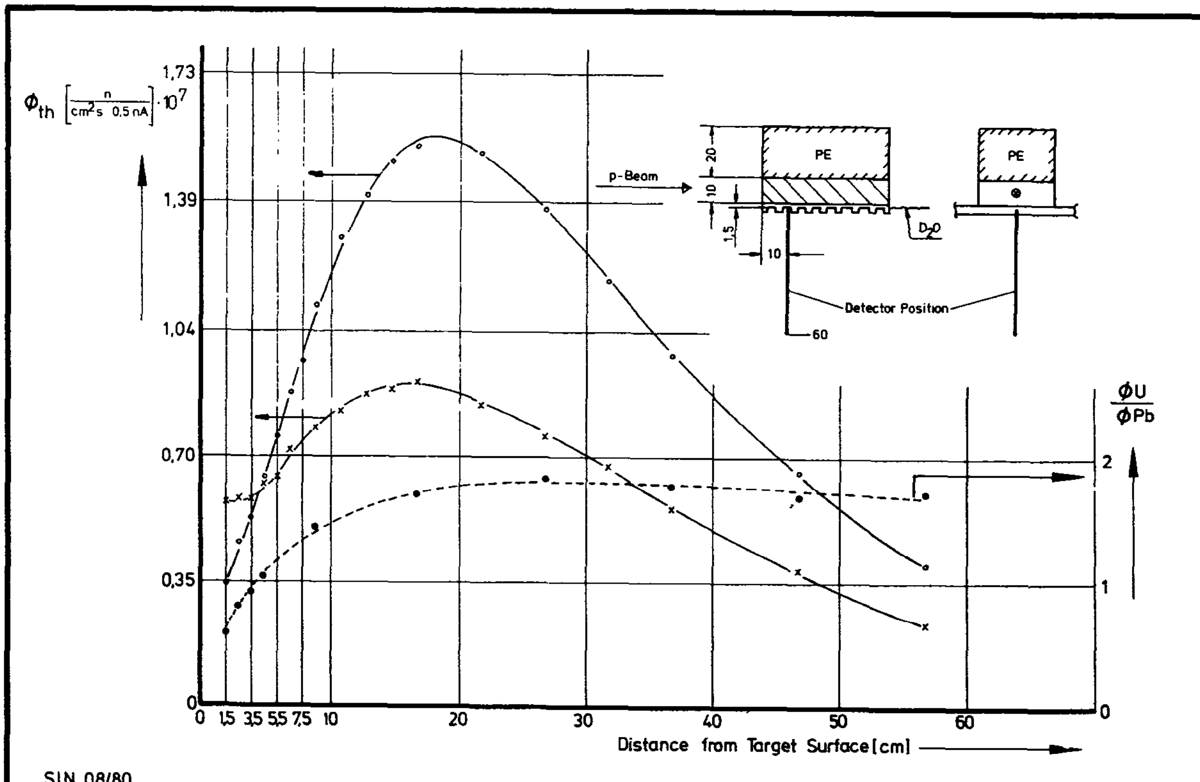

KFA

Termal Flux in D_2O
x——x Pb-Target
o——o U-Target
●- - - -● $\frac{\phi U}{\phi Pb}$

Fig.: 8

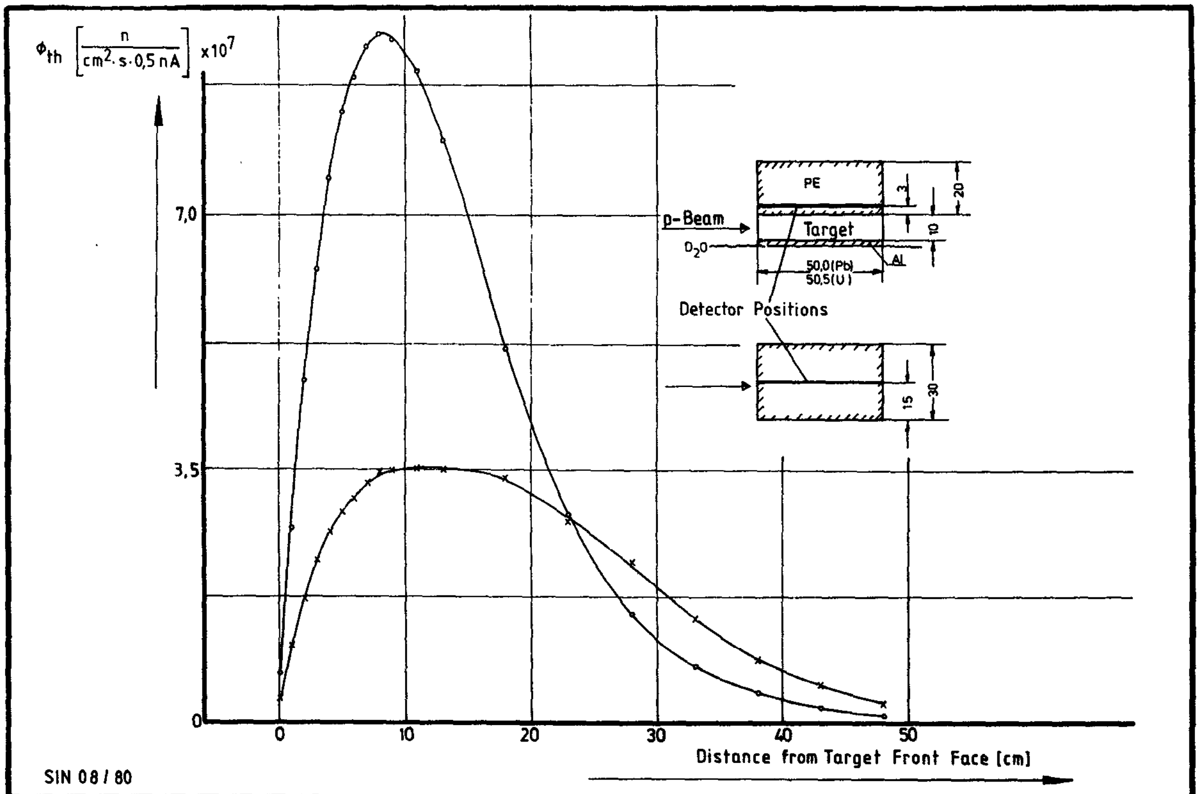

Thermal Flux in PE
×——× Pb-Target
o——o U-Target

Fig.: 9

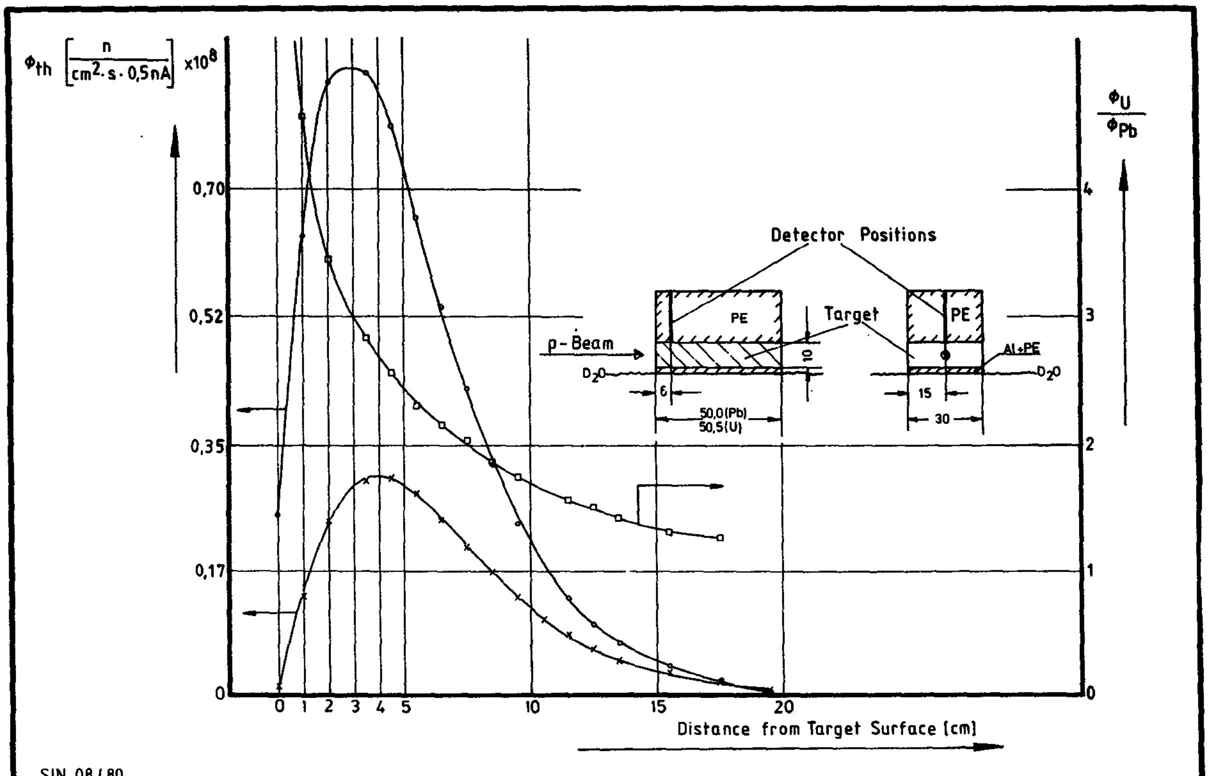

Thermal Flux in PE
×——× Pb-Target
o——o U-Target □——□ $\frac{\Phi_U}{\Phi_{Pb}}$

Fig.: 10

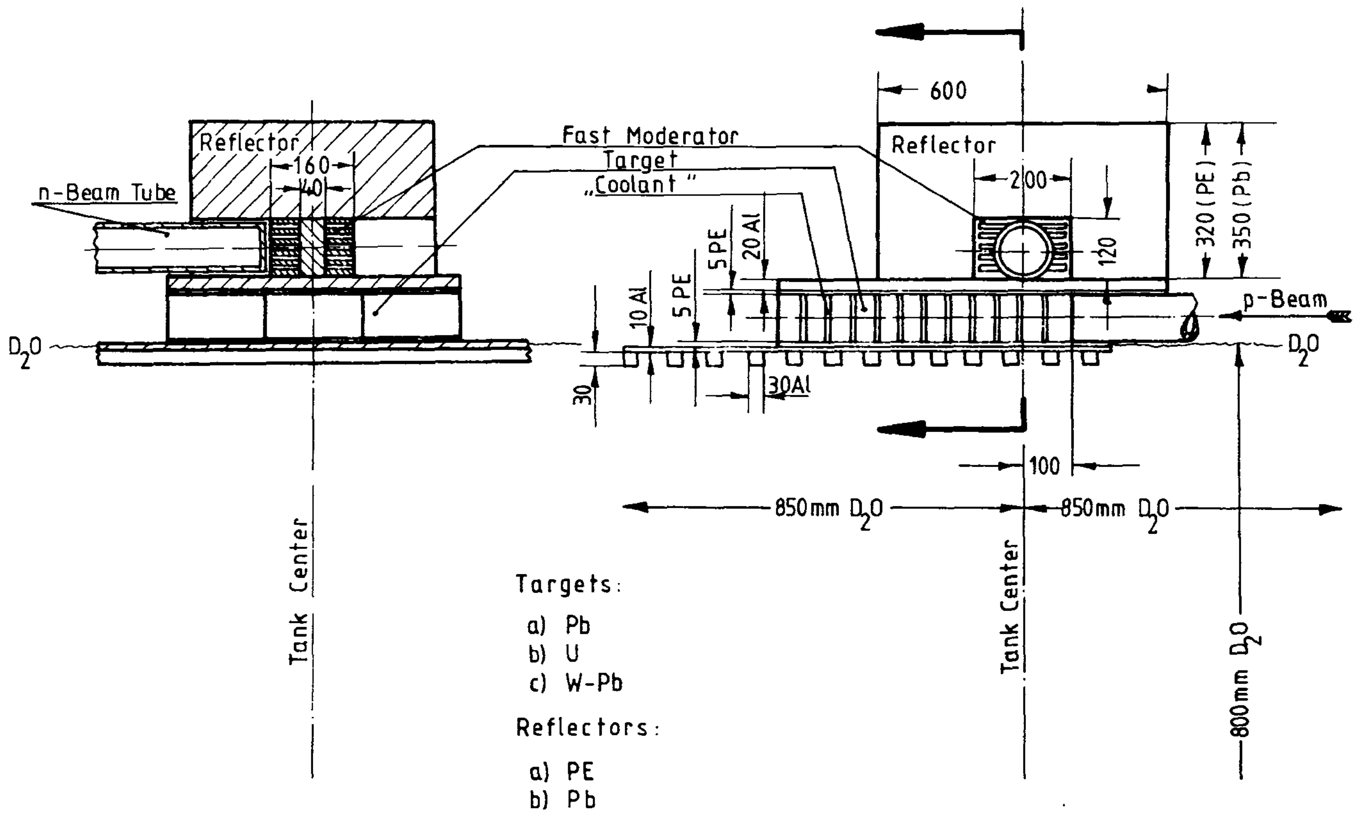

Mock up Assembly of the SNQ Design Fig.:11

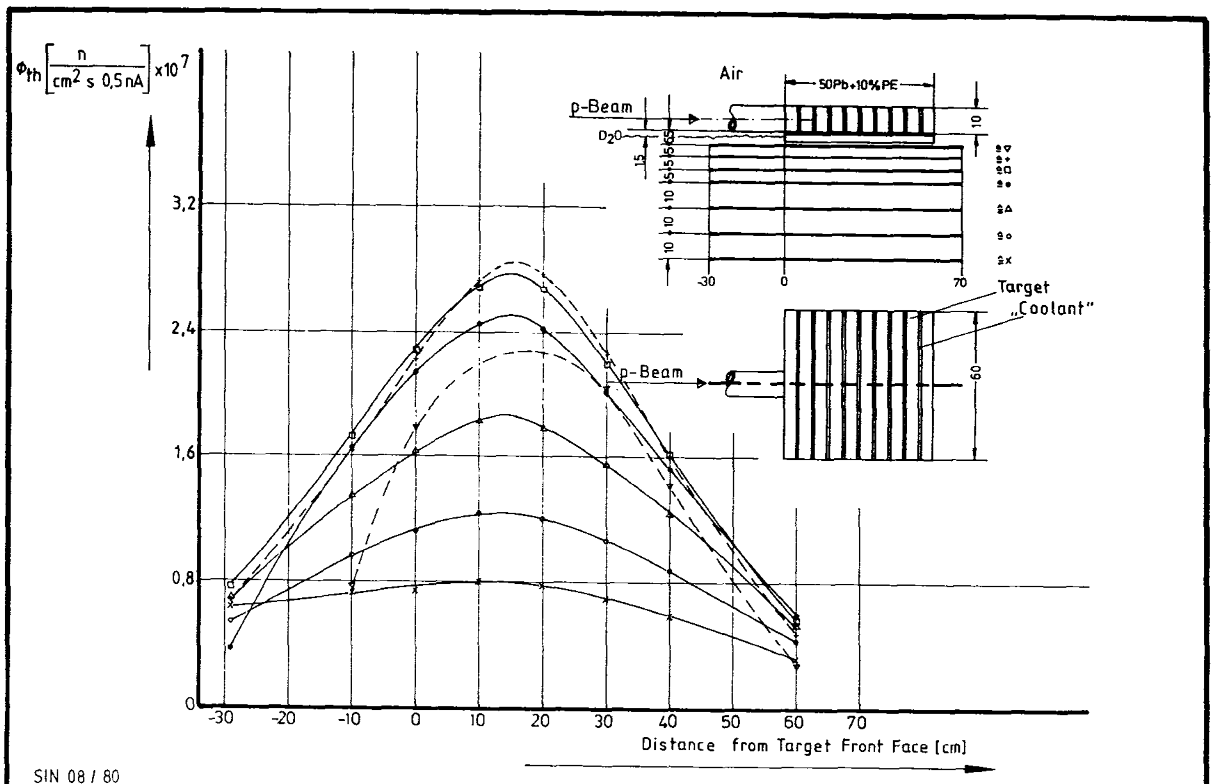

KFA

Thermal Flux in D_2O, Hybridsystem, Pb-Target, Slab with „Coolant"

Fig.: 12

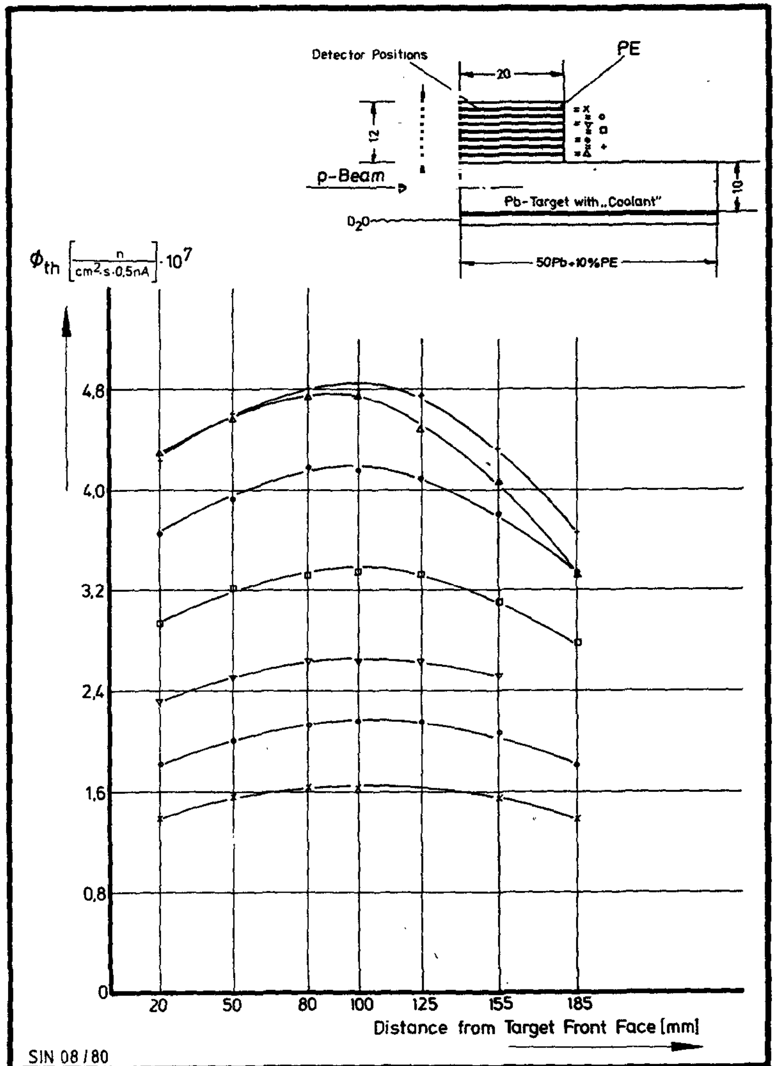

KFA | Thermal Flux in PE, Hybridsystem, Pb-Target, Slab with „Coolant" | Fig.: 13

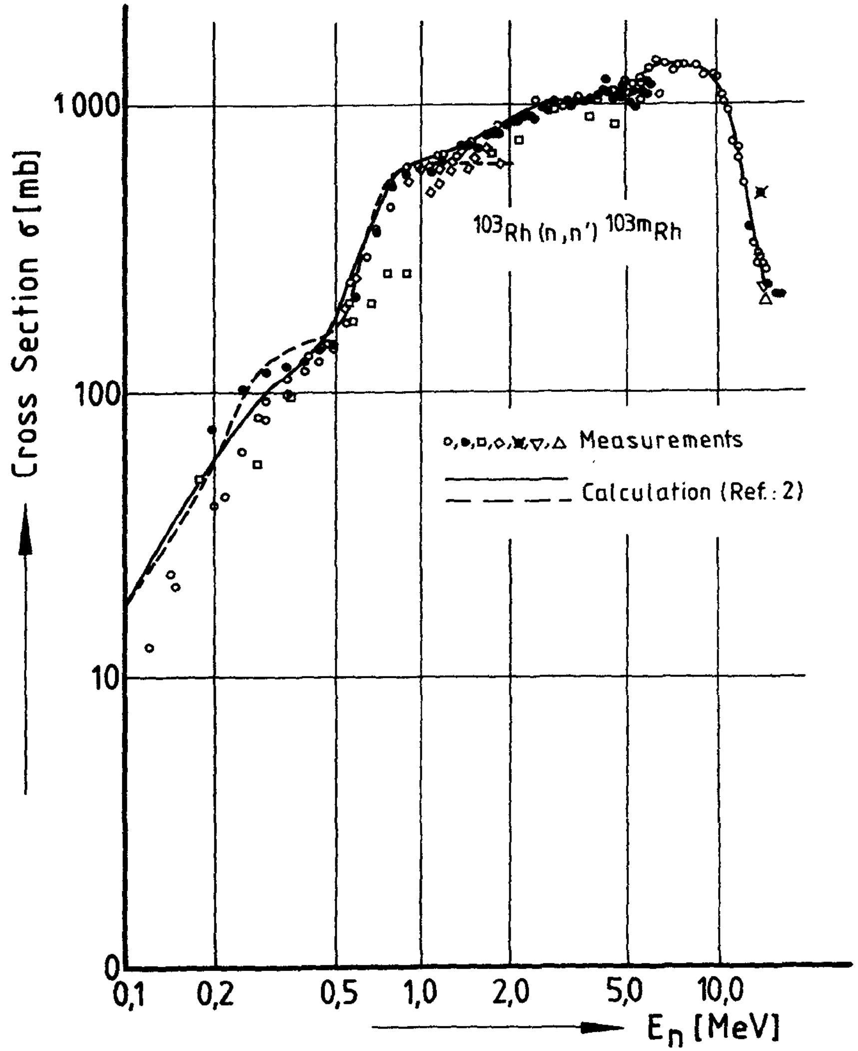

Inelastic neutron scattering cross section of ^{103}Rh

Fig.: 14

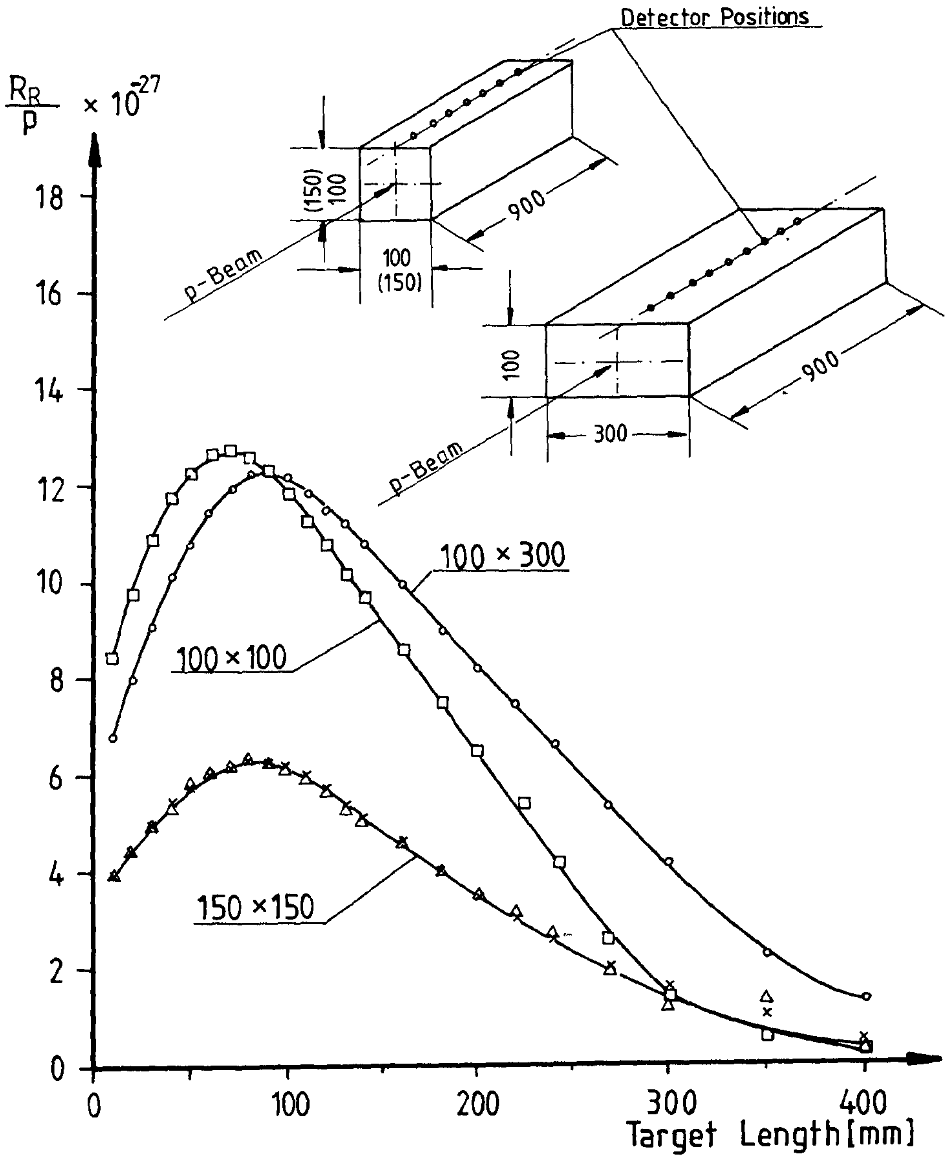

Absolut Rh-Reaction Rate Pb-Target, 600 MeV-Proton Energy, Different Target Dimensions

Fig.: 15

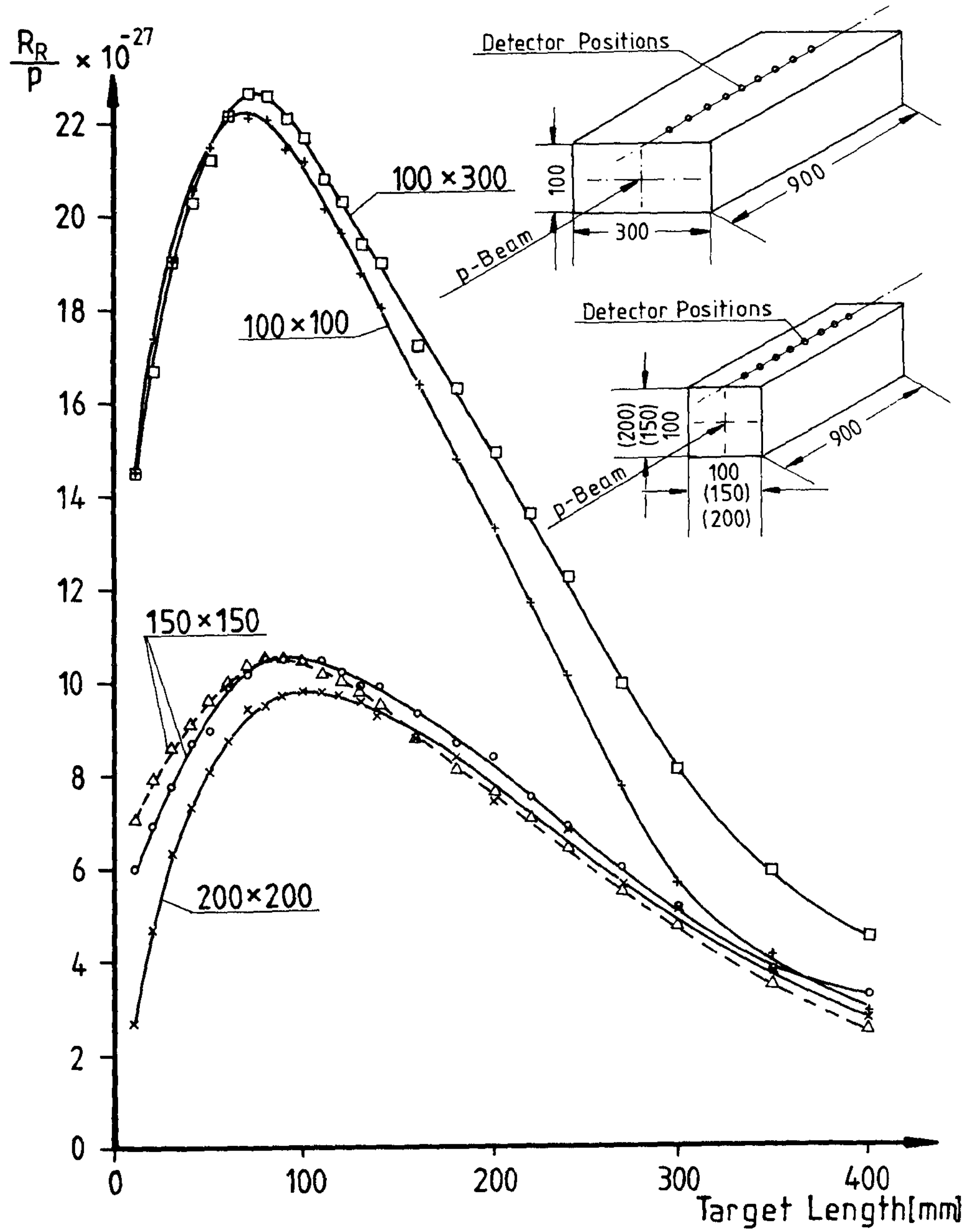

Absolut Rh-Reaction Rate Pb-Target, 1100 MeV-Proton Energy, Different Target Dimensions

Fig.: 16

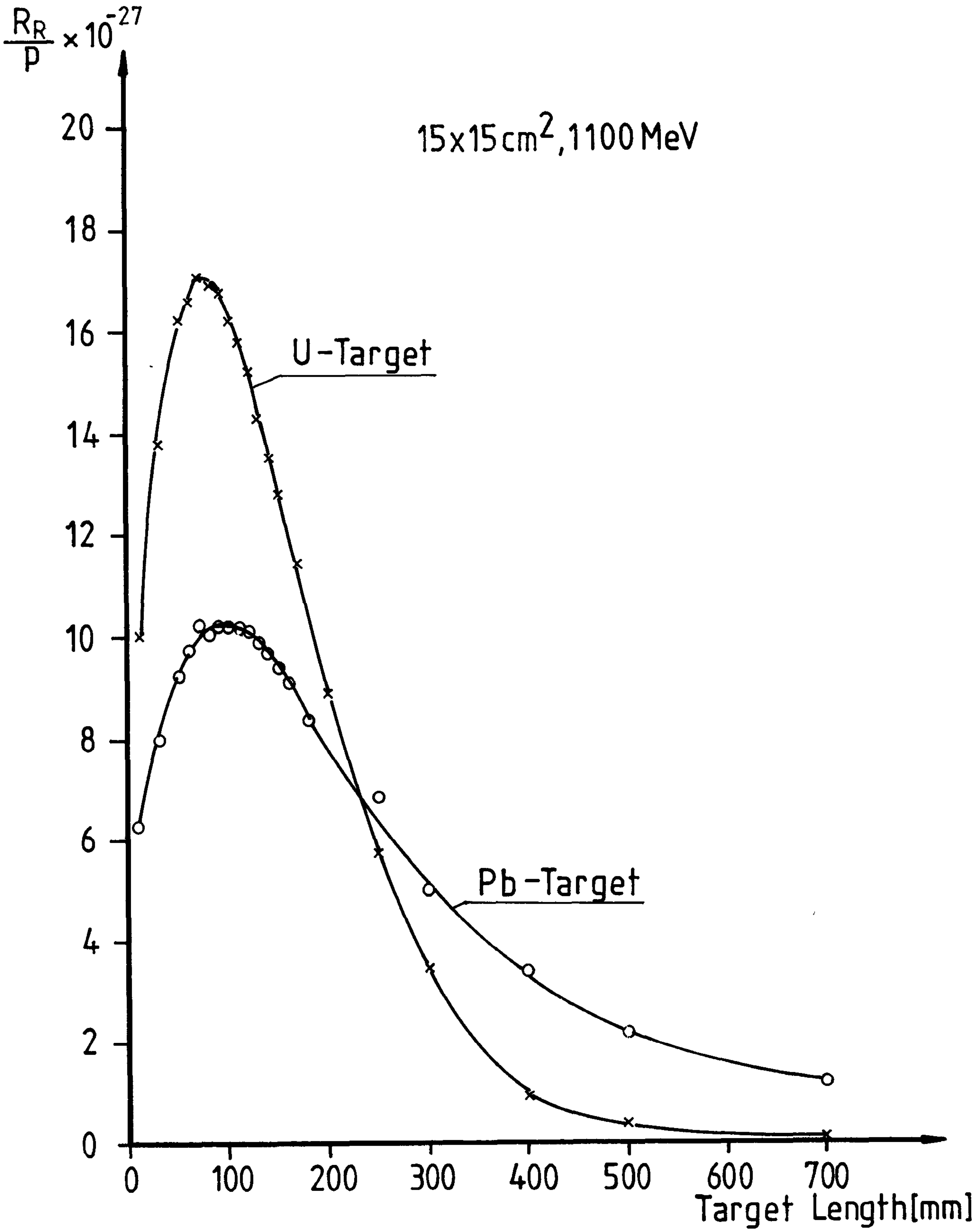

Absolut Rh-Reaction Rate normalized
to one incident Proton

Fig.: 17